

Cloud Ensemble Simulation with the July 1995 IOP Data

K.-M. Xu

*Department of Atmospheric Science
Colorado State University
Fort Collins, Colorado*

Introduction

This study is a part of the Atmospheric Radiation Measurement (ARM) Program single-column model (SCM) intercomparison project, which compares the performance of various SCMs and cloud ensemble models (CEMs) with ARM intensive observation period (IOP) data sets. The goal of this project is to improve the representations of cloud formative/dissipative processes in general circulation models (GCMs). The approach of SCMs and CEMs for achieving such a goal has been reviewed by Randall et al. (1996).

A CEM resolves individual clouds and their mesoscale organization but covers a large horizontal domain. It allows several clouds of various sizes to develop simultaneously and randomly inside the model domain. Thus, the major difference between an SCM and a CEM is that cloud processes are explicitly resolved in a CEM, but must be parameterized in an SCM. On the other hand, CEMs have their own parameterizations such as turbulence closure, cloud microphysics, and radiative transfer. There are still some uncertainties in CEMs, but they are not involved with cloud-scale processes that have to be parameterized in an SCM. Thus, CEMs can be used as a valuable tool for SCMs to achieve the goal of improving cloud parameterizations in GCMs (Randall et al. 1996).

The main objectives of this study are 1) to evaluate the performance of the CEM against the July 1995 IOP observations, 2) to compare the two forcing methods and two analyses of the same data set, and 3) to examine the similarities and differences of midlatitude and tropical cumulus convection. Xu and Randall (1996) simulated tropical cumulus convection in the eastern tropical Atlantic region. Some results from that study will be used in the present study.

Experimental Design

Two sets of simulations were performed with different methods of prescribing the observed large-scale forcings (Krueger and Cederwall 1997). One set of simulations (A,

B, and Q) used the conventional Barnes (1964) objective analysis of the July 1995 IOP data set, performed by Cederwall's group at Lawrence Livermore National Laboratory (LLNL); for simplicity, the LLNL analysis. Another set of simulations (D, E, and F) used the constrained variational analysis performed at the State University of New York-Stony Brook (SUNY-SB) by Ming-hua Zhang (the Zhang analysis). In simulations A and D, the observed total (horizontal plus vertical) advective forcings are prescribed. The vertical velocity and the horizontal advective forcings are prescribed in simulations B and E. In C and E, a nudging procedure was adopted, which will not be discussed in this study.

The UCLA/CSU CEM

The University of California at Los Angeles/Colorado State University (UCLA/CSU) CEM (Krueger 1988, Xu and Krueger 1991, Xu and Randall 1995) is used in this study. Briefly, the CEM is based on the anelastic system of dynamical equations with the Coriolis acceleration. The parameterizations of the model include 1) a third-moment turbulence closure (Krueger 1988), 2) a three-phase bulk cloud microphysics (Lin et al. 1983, Lord et al. 1984, Krueger et al. 1995), and 3) an interactive radiative transfer (Harshvardhan et al. 1987, Xu and Randall 1995).

Some aspects of the model designs that may impact simulated results are 1) the periodic lateral-boundary conditions, 2) the zero terminal velocity for ice crystals, 3) the lack of horizontal advection of condensates, 4) the lack of subgrid-scale cloudiness parameterization, and 5) the method of prescribing large-scale advective effects. These aspects have been explained by Xu and Randall (1996). Only the last aspect will be further addressed in this study.

Results

Comparison Between Analyses

Runs B and E are first presented to compare the performance of the CEM with the two different analyses of the July 1995 IOP data. Briefly, the results from these two

runs exhibit many similarities and differences, in addition to their overall agreement with observations.

Specifically, the simulated surface precipitation rates in Run B and E agree with observations very well (Figure 1), except for the first half of the IOP for Run B. This is not surprising because the Zhang analysis employed the moisture budget balance, whereas the LLNL analysis did not.

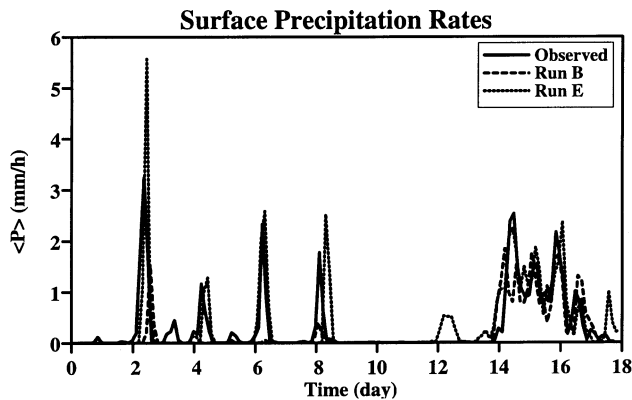


Figure 1. Time series of observed and simulated surface precipitation rates, starting from 00Z July 18, 1995.

The simulated precipitable water (Figure 2) shows more significant differences between the two runs. Only Run E agrees with observations very well. Such differences have great impacts on the surface radiative budget. In addition, the differences shown in Figures 1 and 2 are much greater than those with different forcing methods (not shown), i.e., uncertainties in analyses are much greater and need to be improved.

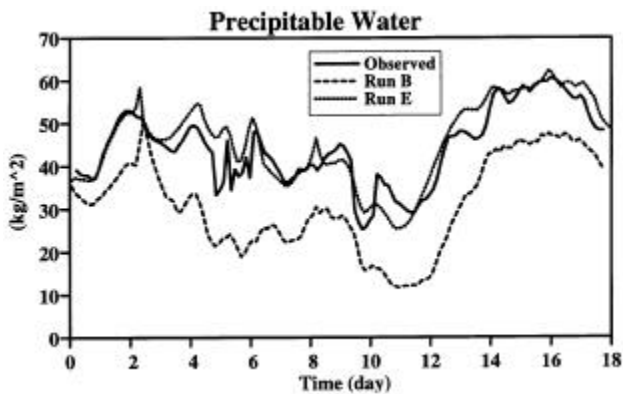


Figure 2. As in Figure 1 but for the domain-averaged precipitable water.

On the other hand, the outgoing longwave radiation (OLR) fluxes in Run B agree with observations slightly better than Run E (Figure 3). This is somewhat surprising. A careful examination reveals that upper tropospheric clouds are better simulated in Run B (not shown). This suggests that the LLNL analysis has its strength. Its weakness is related to the simulated intensity of cumulus convection and soundings.

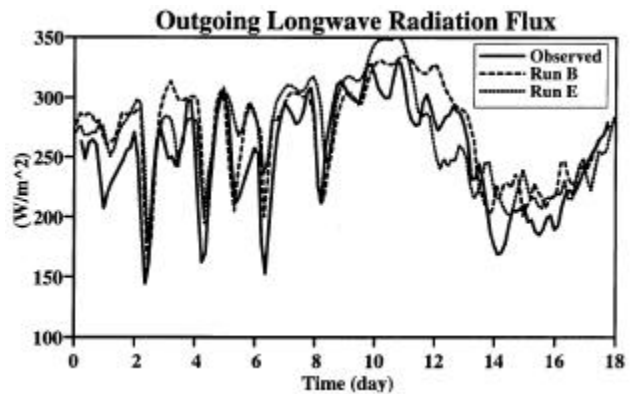


Figure 3. As in Figure 1 but for the OLR fluxes.

The agreement of soundings between observations and simulations is presented with the correlation coefficient (Figure 4) and the root-mean-square (rms) error (Figure 5). The correlation coefficient for moisture is mostly in the

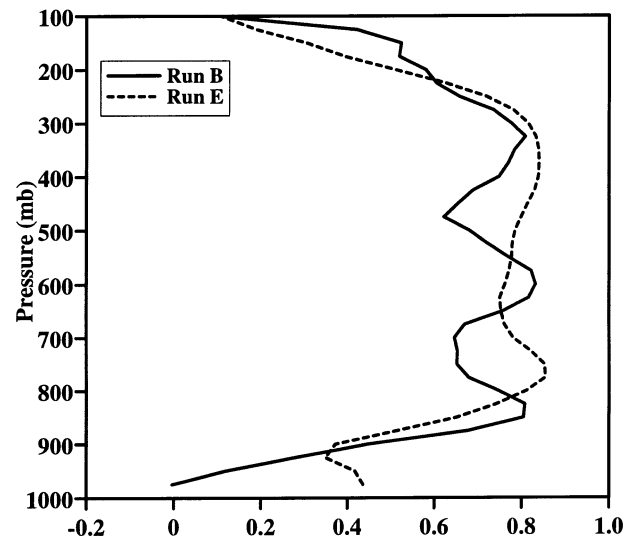


Figure 4. Vertical profiles of correlation coefficient of water vapor mixing ratio between observations and simulations.

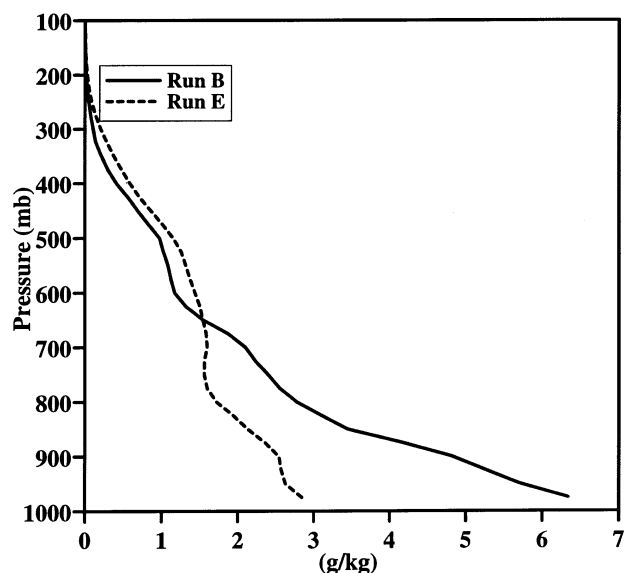


Figure 5. As in Figure 4 but for rms errors from observations of water vapor mixing ratios.

range of 0.6 to 0.8 in either run. However, the rms error in Run B is much greater than in Run E because of large underestimates in Run B (also see Figure 2). For temperature (not shown), the correlation coefficient is smaller and varies greatly with height (0.3 to 0.9). The rms errors are mostly between 1.5 K and 3 K, which are much smaller than those from SCMs.

In summary, the different analyses of the July 1995 IOP data set are used in the CEM simulations. The results show many similarities, but the differences are not negligible at all.

Comparison Between Forcing Methods and with Tropical Cumulus Convection

The new set of comparisons will be focused on 1) quantities related to the intensity of cumulus convection and 2) between Runs D and E. Statistical properties of CEM simulated, tropical cumulus convection (Xu and Randall (1996) are also compared.

The temporal averaged profiles of apparent heat source (Q1) and apparent moisture sink (Q2; Yanai et al. 1973) are first compared with observations for those periods with observed surface precipitation rates over 0.1 mm h^{-1} (Figure 6). The agreements between observations and simulations (D and E) are, as expected, remarkable. The apparent heat source profile shows a maximum at 400 mb and a minimum at 900 mb, while that of Q2 shows double maxima at 900 mb

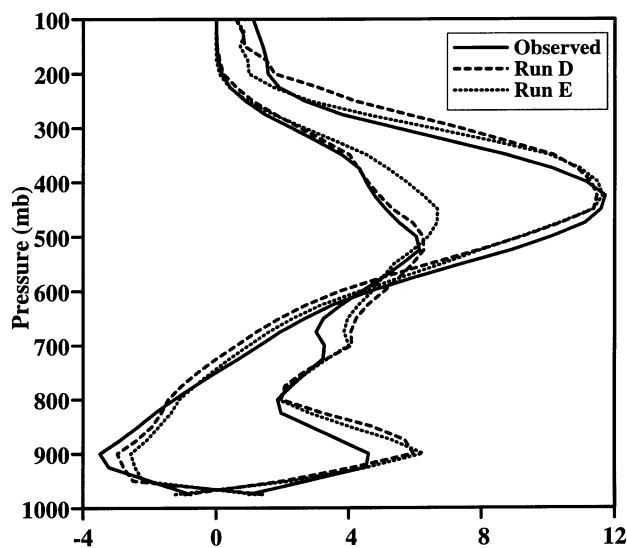


Figure 6. Vertical profiles of Q1 and Q2 for convectively active periods of the 10P, observed versus Runs D and E.

and 500 mb, respectively. The differences between simulation and observation are slightly larger in Run E than in Run D at selected levels. The correlation coefficients between simulated and observed Q1 (Q2) are also slightly higher in Run D (not shown), i.e., around 0.7 above 800 mb. These are due to the fact that the feedback of the domain-averaged soundings on the vertical advective forcings is allowed in Run E.

The differences of midlatitude from tropical cumulus convection are distinct (Figures 6 and 7); i.e., 1) apparent cooling below 700 mb, 2) large apparent drying around 500 mb, and 3) higher locations of Q1 and Q2 maxima. These differences are due solely to the land-ocean contrasts. For example, the lower troposphere in the midlatitude is much drier, which is favorable for evaporation; i.e., producing cooling and moistening. The diurnal variation of surface turbulence fluxes in the midlatitude is much greater than in the Tropics. This favors locally driven convection. On the other hand, similarity between midlatitude and tropical cumulus convection is undeniable. The difference of Q1 and Q2 is positive in the middle and upper troposphere, but negative in the lower troposphere. Such a feature is related to the vertical profiles of the moist static energy and the associated convergence of eddy transports. The convergences of eddy heat and moisture fluxes (not shown) are rather similar between tropical and midlatitude convection throughout the troposphere except for the lowest 200 mb. The turbulent contributions to the convergences are constrained to the lowest 50 mb in the Tropics, but

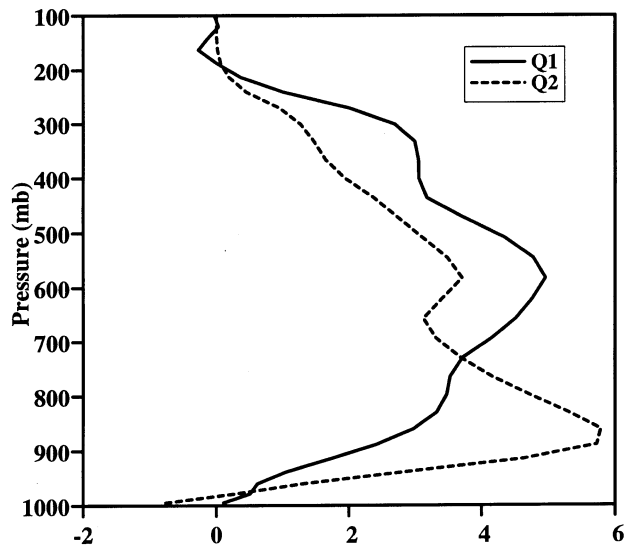


Figure 7. Vertical profiles of Q1 and Q2 for the GATE simulation G (Xu and Randall 1996).

distributed in the lowest 200 mb. This is related to the large variations of the planetary boundary layer depths in the midlatitude.

The cumulus mass flux (Figure 8a) shows appreciable differences between Runs D and E, with smaller peak values in Run D. Similar differences are also apparent in updraft (Figure 8b) and downdraft mass fluxes (Figure 8c). That is, the intensity of cumulus convection is slightly weaker in Run D than in Run E. This difference is deceiving because the 18-day mean surface precipitation rates between the two runs differ by less than 0.02 mm h^{-1} . Because the observed surface precipitation rates are used to classify the convectively active subperiods, the phase differences between simulation and observation can account for the differences seen from Figure 8.

On the other hand, the differences between midlatitude and tropical cumulus mass fluxes are substantially larger, as far as the vertical structures are concerned. In the cumulus mass flux (Figure 8a), downward mass flux is present in the lowest 200 mb in the midlatitude due to the higher subcloud layers. The maximum mass flux is also located in the upper troposphere. This is due to the weak vertical variation of the updraft mass flux above 700 mb (Figure 8b) in the midlatitude. In the Tropics, the largest updraft mass flux are located between 900 mb and 600 mb, in spite of the fact that shallow cumulus clouds were well underestimated in Run G (Xu and Randall 1996). The differences in the downdraft mass fluxes are related to those of the updraft mass fluxes because the downdraft mass fluxes are also larger in the upper troposphere.

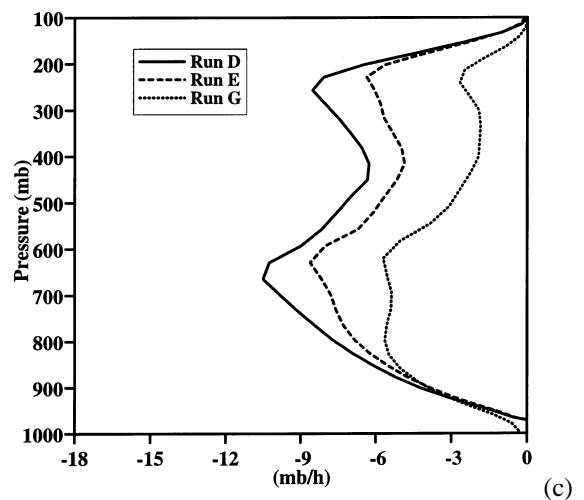
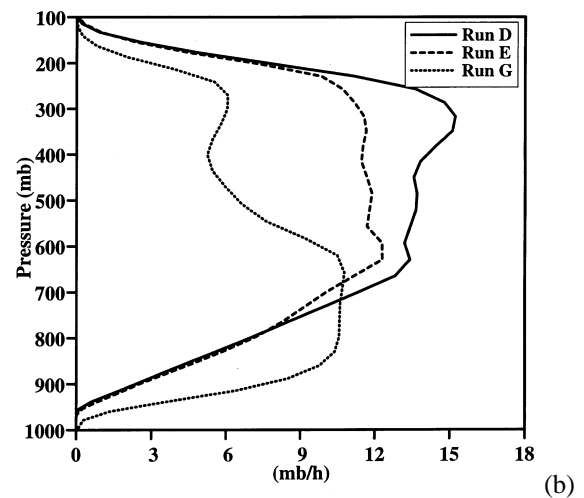
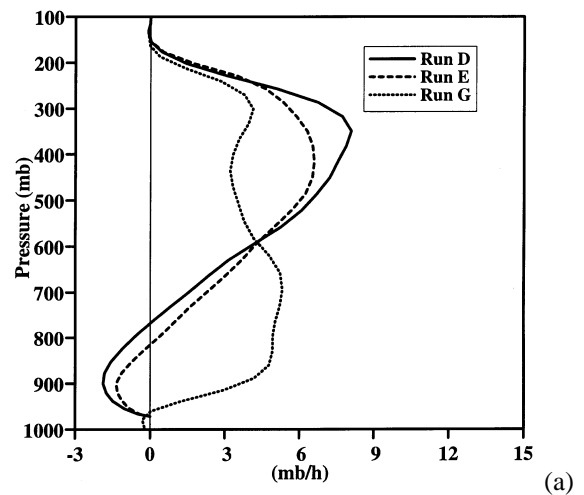


Figure 8. Vertical profiles of (a) cumulus mass flux, (b) updraft mass flux, and (c) downdraft mass flux.

Summary and Conclusions

The results presented in this study can be summarized as follows:

1. The CEM simulated results agree reasonably well with the available observations. The differences between simulation and observation with the ARM IOP data set are, however, larger than those of the Tropics.
2. The two analyses of the July 1995 IOP data set have different strengths and weaknesses for simulating the statistical properties of cumulus convection in the midlatitude with the UCLA/CSU CEM.
3. Different specifications of the large-scale advective forcings in the CEM have some impacts on the simulated results, as far as the July 1995 IOP data set is concerned. However, the impacts are much smaller than those due to different analyses of the same data set.
4. Significant differences exist between tropical and midlatitude cumulus convection, especially in the vertical structures of cumulus mass fluxes, Q1 and Q2.
5. The large variations of the subcloud layers in the midlatitude also impact the convergences of eddy heat and moisture transports and subsequently Q1 and Q2.

Further study is under way to examine the impact of the uncertainties in the observed surface turbulent fluxes on the simulated cumulus convection. Comparison with SCM results will be made to further achieve the goal of the ARM SCM intercomparison project.

Acknowledgments

This research has been supported by the Environmental Sciences Division of the U.S. Department of Energy under grant DE-FG03-95ER61968 as a part of the ARM Program. The computations were performed at the National Energy Research Supercomputer Center, Livermore, California.

References

- Barnes, S. J., 1964: A technique for maximizing details in numerical map analysis. *J. Appl. Meteor.*, **3**, 396-409.
- Harshvardhan, R. Davies, D. A. Randall, and T. G. Corsetti, 1987: A fast radiation parameterization for general circulation models. *J. Geophys. Res.*, **92**, 1009-1016.
- Krueger, S. K., 1988: Numerical simulation of tropical cumulus convection and their interaction with the subcloud layer. *J. Atmos. Sci.*, **45**, 2221-2250.
- Krueger, S. K., and R. T. Cederwall, 1997: ARM single column model working group: SCM intercomparison. Case 1: Summer 1995 SCM IOP. Available from <http://wetfly.llnl.gov/scm/scm-intercomp/>.
- Krueger, S. K., Q. Fu, K. N. Liou, and H.-N. Chin, 1995: Improvements of an ice-phase microphysics parameterization for use in numerical simulation of tropical convection. *J. Appl. Meteor.*, **34**, 281-287.
- Lin, Y.-L., R. D. Farley, and H. D. Orville, 1983: Bulk parameterization of the snow field in a cloud model. *J. Climate Appl. Meteor.*, **22**, 1065-1092.
- Lord, S. J., H. E. Wiloughby, and J. M. Piotrowicz, 1984: Role of a parameterized ice-phase microphysics in an axisymmetric, nonhydrologic tropical cyclone model. *J. Atmos. Sci.*, **41**, 2836-2848.
- Randall, D. A., K.-M. Xu, R. Somerville, and S. Iacobellis, 1996: Single-column models and cloud ensemble models as links between observations and climate models. *J. Climate*, **9**, 1683-1697.
- Xu, K.-M., and S. K. Krueger, 1991: Evaluation of cloudiness parameterizations using a cumulus ensemble model. *Mon. Wea. Rev.*, **119**, 342-367.
- Xu, K.-M., and D. A. Randall, 1995: Impact of interactive radiative transfer on the macroscopic behavior of cumulus ensembles. Part 1: Radiation parameterization and sensitivity test. *J. Atmos. Sci.*, **52**, 785-799.
- Xu, K.-M., and D. A. Randall, 1996: Explicit simulation of cumulus ensembles with the GATE Phase III data: Comparison with observations. *J. Atmos. Sci.*, **53**, 3710-3736.
- Yanai, M., S. Esbensen, and J.-H. Chu, 1973: Determination of bulk properties of tropical cloud clusters from large-scale heat and moisture budgets. *J. Atmos. Sci.*, **30**, 611-627.